Feasibility Study of a Portable Coupled ^{3}He Neutron Detector with $LaBr_3$ Gamma Scintillator for the Purpose of Plutonium Identification and Quantification

Daniel C. Strohmeyer and William S. Charlton

Texas A&M University
Nuclear Security Science & Policy Institute
MS 3473 TAMU
College Station, TX 77845
E-mail: danielstrohmeyer@neo.tamu.edu, charlton@ne.tamu.edu

Abstract:

In recent years there has been several research endeavors to increase the ability to identify and quantify special nuclear material in field measurements. Many have included both gamma spectroscopy and neutron coincidence systems that are portable and work in a variety of environments. In this work a MCNPX[1] model was designed that includes four gamma detection slabs placed within four neutron detection slabs. Four Plutonium (Pu) samples of known quantity were modeled and tested to determine what data was available from each individual signature. Each model included a separate MCNPX deck for each individual isotope that contributes to the gamma signature in photon mode and a spontaneous fission and (α,n) deck for the neutron signature. The first three samples were used to create spectrums and efficiency curves for each odd isotope as well as for a Pu effective mass for the neutron signature. The data from these simulations were then used to identify the isotopics in the fourth sample to within acceptable accuracy. From this data a total Pu mass was obtained as well as an ability to determine the ratio of (α,n) to spontaneous fission neutrons without additional simulations. This provides a new method to detected and identify the Pu content within a sample without producing additional information since isotopics can be determined with the use of the gamma and neutron system.

Keywords: neutron coincidence counting, gamma spectroscopy, plutonium identification and quantification

1. Introduction

Neutron coincidence counting has been available for many years and is a well established method to quantify special nuclear material. However, there are limitations to its applications. The most notable of these is the requirement to know the isotopics of the sample being measured. The purpose of this work was to study the advantages of using a coupled neutron and gamma measurements in a single field deployable detector system over currently available portable neutron coincidence counters. The system of interest should be portable so that it can work in a number of environments. It should also have a small foot print to minimize the space required. Coupled neutron and gamma measurements have been studied previously[2,3]; however, this work focused on a portable system using an advanced γ-spectroscopy system[4] which would be field deployable. The feasibility of this design concept was studied using MCNPX simulations.

2. Theory

The material of interest in this work is special nuclear material but we will focus primarily on PuO_2. PuO_2 emits neutrons due to spontaneous fission (SF) and (α,n) reactions. It also emits characteristic γ-rays that are produced in coincidence with α-emissions. The neutrons and gammas travel at different speeds and therefore are detected at different times within the detector.

2.1 Coincidence counting

There are several different types of coincidence counters available today of various shapes, sizes, and efficiencies. Many consist of a slab or well design and operate with efficiency generally above 20%, but most of these systems are not easily movable. They tend to be heavy and cumbersome and are not able to be used in the field.

A coincidence counter determines Pu mass in the sample by measuring the singles or totals and doubles or reals (coincident) neutrons that are produced by (α,n) and spontaneous fission. The totals (T) and reals (R) count rates are given by the so-called Neutron Coincidence Point Model[5]:

$$T = m_{240}^{eff} Y_{240} \epsilon M \nu_{s1} (1 + \alpha) \quad [1]$$

$$R = m_{240}^{eff} Y_{240} \epsilon^2 \frac{\overline{\nu(\nu - 1)}}{2} F \quad [2]$$

$$\overline{\nu(\nu - 1)} = M^2 \left[\frac{\nu_s(\nu_s - 1)}{1 + \alpha\nu_s} + \frac{M - 1}{\nu_I - 1} \frac{1 + \alpha}{1 + \alpha\nu_s} \nu_s \overline{\nu_I(\nu_I - 1)} \right] \quad [3]$$

where m^{eff}_{240} is the $^{240}Pu_{eff}$ mass, Y_{240} is the specific spontaneous fission rate for ^{240}Pu (in fissions/sec/g), F is the doubles gate fraction, ε is the detector efficiency, M is the sample self-multiplication, α is the ratio of neutrons produced from (α,n) reactions to those from spontaneous fission reactions, and $\nu_s(\nu_s\text{-}1)$ and $\nu_i(\nu_i\text{-}1)$ are the factorial moments of the spontaneous fission and induced fission neutron distributions. The ^{240}Pueff mass is the exact mass of ^{240}Pu that would create the same totals and reals count rate as would be measured from the actual sample. The ^{240}Pueff mass (m^{eff}_{240}) is given by:

$$m_{240}^{eff} = 2.52 m_{238} + m_{240} + 1.68 m_{242} \quad [4]$$

where m_{238} is the ^{238}Pu mass in the sample, m_{240} is the ^{240}Pu mass, and m_{242} is the ^{242}Pu mass. The total Pu mass is given by

$$m_{Pu} = m_{238} + m_{239} + m_{240} + m_{241} + m_{242} + m_{Am241} \quad [5]$$

where m_{239} is the ^{239}Pu mass in the sample, m_{241} is the ^{241}Pu mass, and m_{Am241} is the ^{241}Am mass. Thus to get the total Pu mass the isotopic ratio of the Pu is needed. For an unknown sample in the field, this quantity would not necessarily be known. The ε, F, $\nu_s(\nu_s\text{-}1)$ and $\nu_i(\nu_i\text{-}1)$ are known for samples of unknown mass and isotopics. The values for m^{eff}_{240}, M, and α are unknown. This leaves two equations with three unknowns. Therefore, at least one of the unknowns must be determined by an alternate means. Typically M or α are calculated on assumptions about the sample isotopics and/or geometry.

2.2 Gamma detection

There are many different types of γ-spectroscopy systems currently used. The two main ones are solid-state and scintillation systems. They both have advantages and disadvantages. High Purity Germanium (HPGe) is the most common solid-state detector available and has the best resolution available on the market today. This resolution comes at a cost of portability since it has to be kept at liquid nitrogen (LN) temperatures for proper function. There are portable systems available but these have some limitations.

Scintillation detectors, most commonly Sodium Iodide (NaI)[7], are generally much more portable than HPGe but have a lower resolution. They are also much more rugged, can operate at room temperature, have higher efficiency, and are available in larger crystals than HPGe. In recent years, there has been a tremendous amount of research to improve the resolution of scintillation detectors. One of the most notable advancements is the use of Lanthanum Bromide ($LaBr_3$) crystals. $LaBr_3$ has superior resolution to NaI (though still less than HPGe). Also in recent years, the development of nanocrystals embedded in a clear matrix has been developed at LANL using $LaBr_3$ crystals as the scintillation material[4]. This should be able to increase the available crystal size and provided alternate variations in geometry.

3. MCNPX benchmarking

Since nanocrystals detectors are still under development and unable to be obtained, an alternate system was modeled in order to validate the usage of MCNPX for $LaBr_3$ crystals. For this, the Canberra IPROL-1 probe (Figure 1) that works with the Inspector 1000 portable gamma spectroscopy system was chosen. The probe was modeled in MCNPX. The model included the crystal, crystal housing, photomultiplier tube, electronics portion, and casing. This model can be seen in Figure 2. The MCNPX simulation included an F8:p pulse height tally with a 4000 bin energy grid to simulate a pulse height spectrum. A Gaussian Energy Broadening (GEB) function[1] was included to appropriately broaden the peaks with FWHM values versus energy measured using a number of sources.

Figure 1. Image of IPROL-1 $LaBr_3$ probe

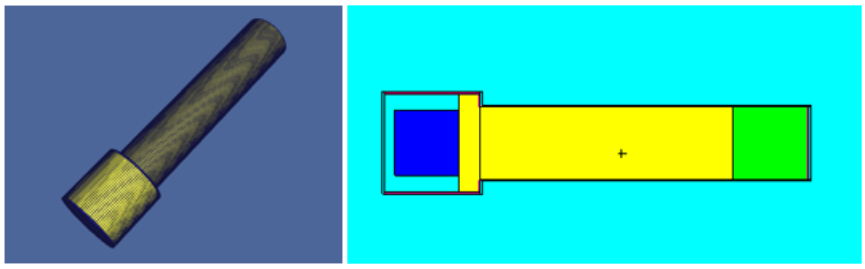

(A) (B)

Figure 2. MCNPX model probe (A) 3-D visualization (B) cross-sectional view

The spectrum from a ^{137}Cs standard was acquired using the IPROL-1 probe. This experiment was then simulated using the MCNPX model. Figure 3 shows the measured and the MCNPX simulated spectra for the ^{137}Cs source. As can be seen, the ^{137}Cs photopeak agreement between the measured and simulated results is generally quite good. However, the agreement in the Compton background and the peaks at 1.435 MeV is poor. This is due to the "internal" background in the detector due to its natural radioactivity.

Natural La contains a small amount of ^{138}La which decays by electron capture with a 1.435 MeV gamma 66.40% of the time and by beta (β) decay with a 788 keV γ and a 252 keV β 33.60% of the time. When both modes of decay are included the 1.435 MeV peak was simulated correctly. The broad plateau between 788 keV and 1040 keV was due to the β particle and the 788 keV γ being detected in coincidence. The β decay produces a continuous energy spectrum; this in essence will nonsymmetrically broaden the 788 keV photopeak. The gamma can also undergo Compton scattering causing the lower energy γ to be detected in coincidence with the β. If the γ escapes entirely just the β detected. These possibilities were accounted for in the simulated spectrum by including the continuous β spectrum in the probability of detection produced by the output of the F8:p tally for every energy bin from E_{bin} to $E_{bin+252\ kev}$ until 788 keV plus 252 kev[7,8,9]. This produced a spectrum that broadened the 788 keV peak and continuum to better represent the actual spectrum. The corrected spectrum is labeled "Corrected MCNPX" in Figure 3.

To confirm the proper simulation of the impact of the La internal radioactivity on the spectrum, a measurement and a simulation of the background only (i.e. without a source present) was performed. The measured and "Corrected MCNPX" spectra for this background is shown in Figure 4. These results were used to develop the procedure for the modeling the $LaBr_3$ detector in the coupled neutron-gamma detector concept being considered here.

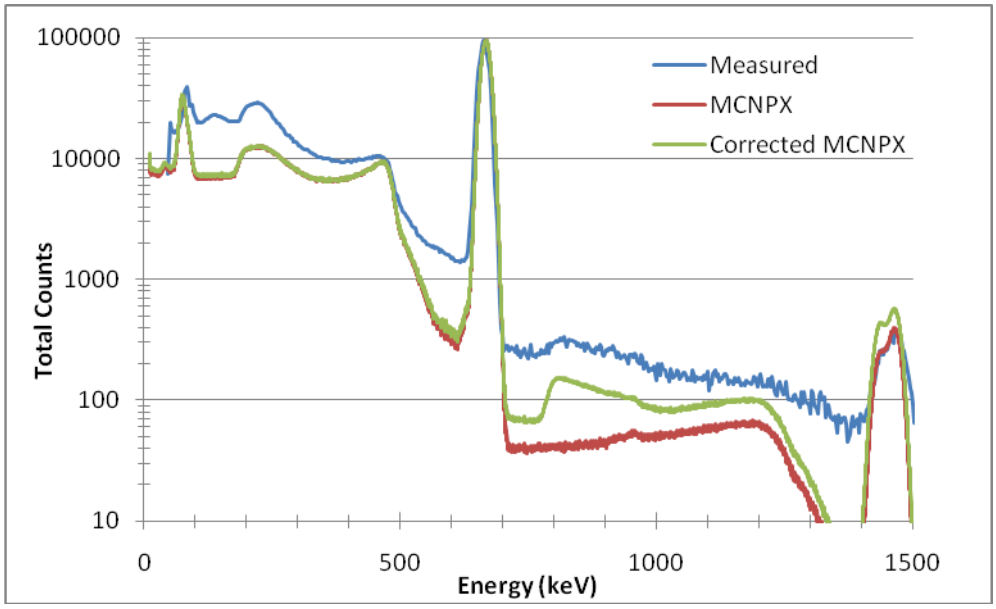

Figure 3. Measured and simulated spectrum for ^{137}Cs for $LaBr_3$ probe

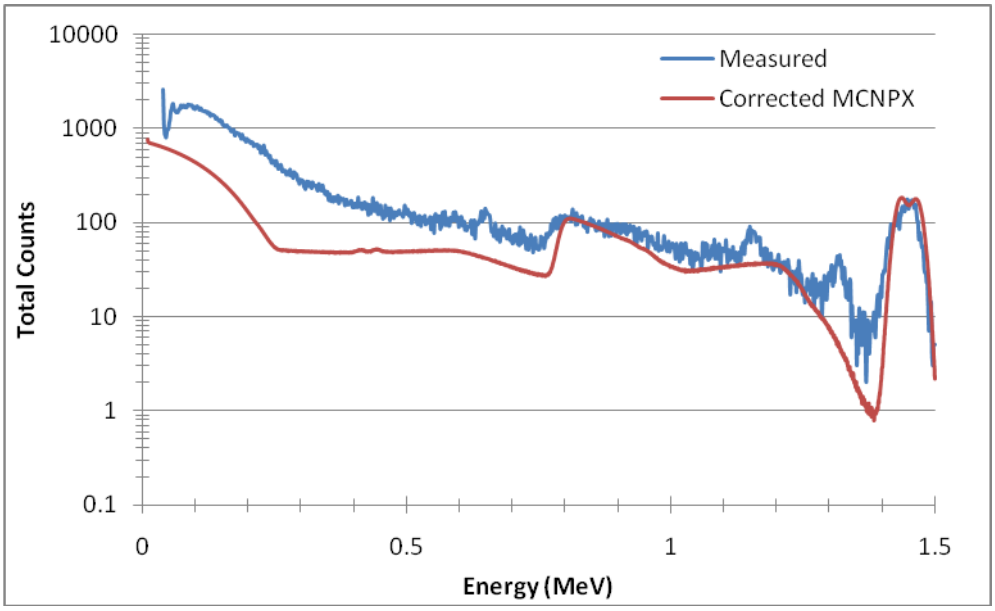

Figure 4. Measured and simulated for the $LaBr_3$ probe background spectrum

4. Simulations and Results

The detector concept consisted of 4 neutron detecting slabs and 4 gamma detection slabs. Each neutron detection slab contains 4 ^{3}He tubes of 2.54 cm OD with a 25.4 cm active length placed within a polyethylene slab[6]. Each gamma detection slab has 2.54 cm of scintillation material, a PMT placed on top, and a 1 mm aluminum casing. The gamma detection slab consisted of an Oleic acid matrix with 50% loading of $LaBr_3$ nanocrystals.[4] The detector concept is shown in Figure 5.

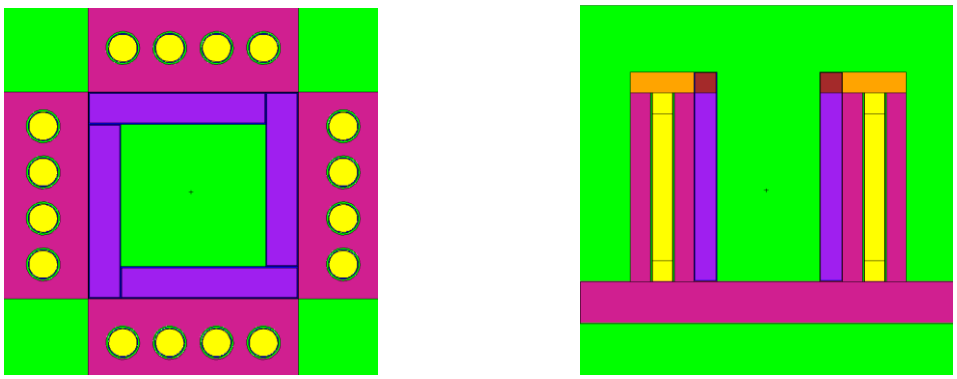

(A) (B)

Figure 5. Detector geometry (A) overhead view (B) cross-sectional view

The four samples listed in Table 1 were used to test the feasibility of this detector design concept. The samples consisted of a PuO_2 powder. Each sample had the same radius but had variations in fill height. The gamma and neutron simulations were executed separately.

Table 1. Detailed sample isotopic information

Sample ID	Pu Mass	Pu238	Pu239	Pu240	Pu241	Pu242	Am241	O16
	(g)	(g)	(g)	(g)	(g)	(g)	(g)	(g)
LAO-251	195.00	0.0975	142.1745	28.314	0.7995	0.6045	1.6575	23.01
LAO-252	365.00	0.1825	266.596	52.5965	1.46	1.1315	2.993	43.07
LAO-255	617.00	0.3085	450.41	89.0948	2.468	1.851	5.0594	72.806
LAO-256	436.00	0.218	318.498	62.9148	1.744	1.308	3.488	51.448

4.1 Gamma spectroscopy simulations

A separate deck was created for each isotope in photon mode. Each deck was executed with 1E8 particles, with 4000 energy bins, and a GEB function. Figure 6 is a plot of each individual isotope and Figure 7 is the sample plot imported to Canberra's Genie 2000[10] (Genie) gamma analysis software, both are for LAO-251.

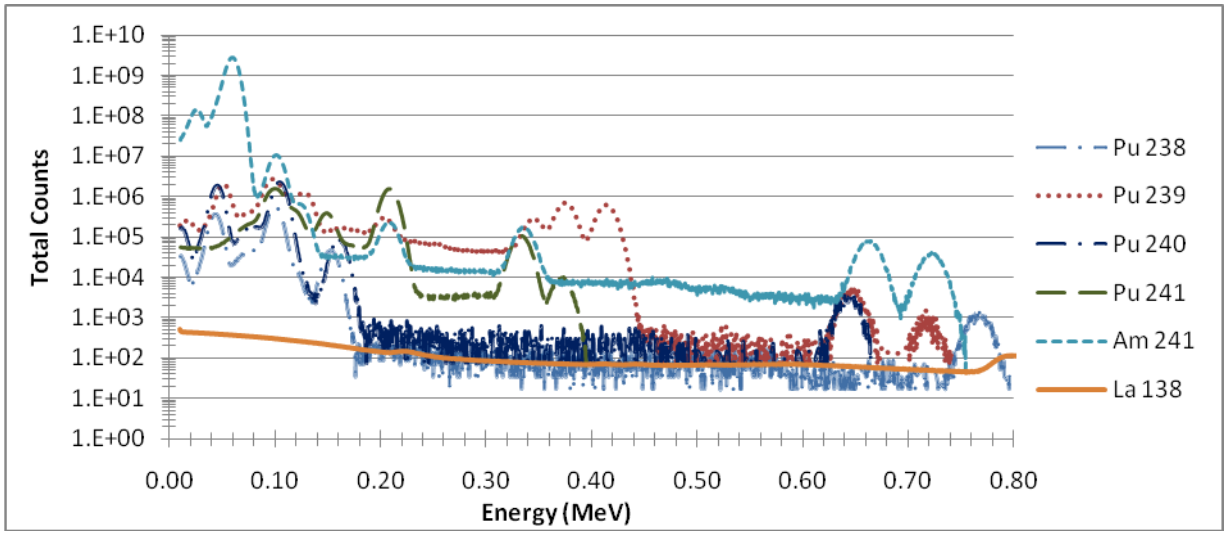

Figure 6. Counts vs. Energy for each individual isotope for $LaBr_3$ detection slab calculated with MCNPX

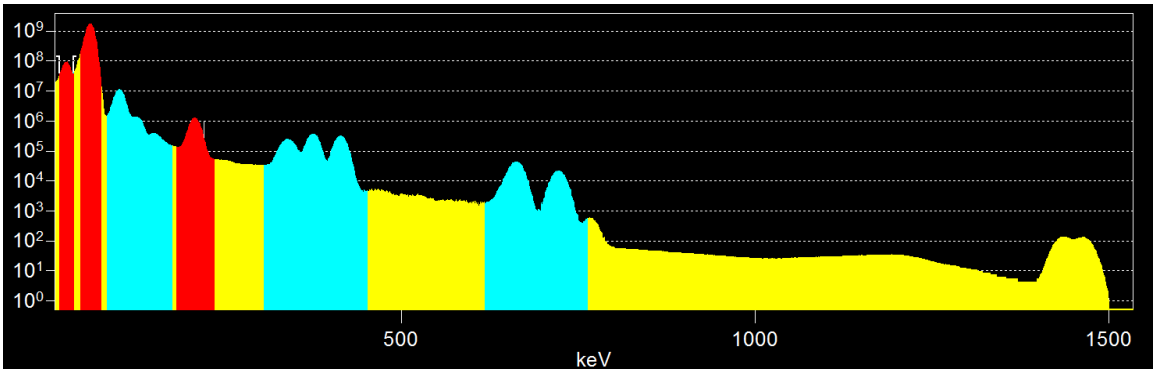

Figure 7. Imported LAO-251 spectrum in Genie 2000

From Figure 6, it can seen that all the isotopes are major contributors to the spectrum below 200 keV, but with the low resolution of $LaBr_3$ these mulitplet peaks are difficult to resolve. Because of this, no peaks in this area were used. A peak analysis was performed of the remaining peaks. It identifies the peaks and provides the net area counts above the continuum. This result provides seven with a range from 208 keV to 766 keV. The values from the efficiencies of the photopeaks can be seen in Table 2. Note that in Figure 7 the 766 keV peak is not highlighted, but was able to be used with Interactive Peak Fit, an analysis tool within Genie.

Table 2. Gamma detection efficiencies

Isotope	Energy	Efficiency		
	(keV)	LAO-251	LAO-252	LAO-255
Pu-241	208.00	10.87%	9.10%	8.01%
Pu-239	375.04	12.18%	12.54%	11.82%
Pu-239	413.17	11.42%	11.92%	11.43%
Am-241	662.42	9.72%	11.43%	11.16%
Am-241	721.99	8.51%	9.88%	9.75%
Pu-238	766.41	7.49%	8.31%	7.86%

4.2 Neutron simulations

For the neutron detector simulations, the same sample geometry was used with two decks for SF and (α.n), respectively. An MCNPX neutron capture tally was used. Each deck was executed for 1E7 histories. A plot of the singles count rate (left axis) and doubles count rate (right axis) versus $^{240}Pu_{eff}$ mass can be seen in Figure 8. In Figure 8 both lines are plotted but are virtually the same value. The associated error from the MCNPX simulation is less that 0.36%.

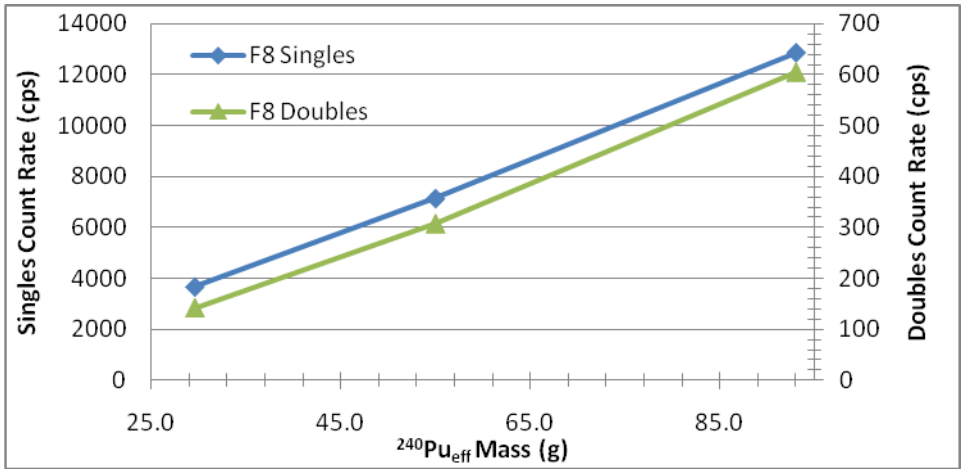

Figure 8. Count rate vs. $^{240}Pu_{eff}$ mass for singles and doubles

4.3 Mass determination

Using the data from both simulations and creating count rate vs. mass plots, similar to Figure 8, a linear relationship can be formed for each gamma peaks in Table 2 and $^{240}Pu_{eff}$ in Figure 8. This allows for equations to be produced that determine the mass of the isotope with only the raw count rate data, meaning no outside information about the sample was used. This provides values for all the masses in Equation 4 and 5 except ^{240}Pu and ^{242}Pu. ^{242}Pu is assumed to be zero based only a minute amount is produced within the sample through absorption. Note that the doubles information was used to calculate $^{240}Pu_{eff}$. This allows ^{240}Pu to be determined through Equation 4. The calculated masses are in Table 3.

Table 3. Calculated vs. Actual isotopic masses

Isotope	Calculated Mass (g)	Actual Mass (g)	Variation
Pu238	0.250	0.218	114.68%
Pu239	314.679	318.498	98.80%
Pu240	62.670	62.915	99.61%
Pu241	1.725	1.744	98.89%
Pu242	0.000	1.308	0.00%
Am241	3.534	3.488	101.33%
$^{240}Pu_{eff}$	63.300	65.612	96.48%

This in turn allows α to be determined which is used within the Neutron Point Model equations previously discussed and is shown in Table 4. Equations 1, 2, and 3 can now be solved as a system of equations.

Table 4. Calculated vs. Actual α value

	Calculated	Actual	Variation
α value	0.522	0.497	104.90%

The calculation yields an M of 1.08224 and a $^{240}Pu_{eff}$ of 60.78 g. The $^{240}Pu_{eff}$ is lower than both the calculation and actual but was expected since M was included in the simulation of MCNPX, but since it was just trying to be done this was disregarded. This shows that the isotopics can be determine with this experiment with little or no information about the sample.

5. Conclusion

Both detector systems are able to be put together and can benefit the other. Before, if a straight neutron count was taken it was required to calculate one of the three unknowns from alternate means, also little to no information is known on the odd isotopes. If just a gamma spectrum was taken it is unlikely that any information would be gathered from the even isotopes. When working together isotopics of the entire sample can be calculated and provide mass and identification of Pu. It could also be used in an environment for any type of nuclide identification. The gamma system has sufficient resolution to identify a number of isotopes, even if no neutrons are present.

There are some draw backs to this system that were unable to be accounted for. The resolution on the $LaBr_3$ slab was the same in this experiment as the probe. This information obtained does not include a

FWHM value, and it was assumed to be the same as the probe, but may not always be the case. Also the total count for the gamma system is extremely high, and most gamma systems used today will not be able to handle a count rate of such magnitude. MCNPX can not include this in the model. This might require that the sample be placed farther away from the detector, which would also affect the neutron count rate. Even with these negative aspects it is still believed that once the gamma detection medium is available the dual use detector system should be explored further and a prototype produced.

6. References

1. MCNPX. Computer software. Vers. 2.5. Los Alamos, NM: Los Alamos National Laboratory.

2. I. Pázsit, L. Pal, A. Enqvist, and S. A. Pozzi, “The Joint Distribution of Detected Neutrons and Gamma Photons from Fissile Samples and its Application in Nuclear Safeguards,” SPIE Fluctuations and Noise, La Pietra Conference Center, Florence, Italy, May 20-24, 2007.

3. A. Enqvist, I. Pazsit, and S. A. Pozzi, “The Detection Statistics of Neutrons and Photons Emitted from a Fissile Sample,” Institute of Nuclear Materials Management Annual Meeting, Tucson, Arizona, July 8-12, 2007.

4. Del Sesto, R. E., E. A. Mckigney, R. E. Muenhausen, K. C. Ott, R. D. Gilbertson, T. M. McCleskey, M. Bacania, L. G. Jacobson, A. K. Burnell, B. L. Bennet, S. C. Sitarz, and J. F. Smith. *Development of Nanocomposite Scintillators*. 2007

5. Reilly, Doug, Norbert Ensslin, and Hastings Smith. Passive Nondestructive Assay of Nuclear Material. Springfield, VA: National Technical Information Service, 1991.

6. Thornton, Angela L. "Development of a Portable Neutron Coincidence Counter for Field Measurements of Nuclear Materials Using the Advanced Multiplicity Capabilities of MCNPX 2.5.F and the Neutron Coincidence Point Model." Thesis. Texas A&M University, 2007

7. Knoll, Glenn F. Radiation Detection and Measurement. New York: Wiley-Interscience, 2000.

8. Cottingham, W. N., and D. A. Greenwood. An Introduction to Nuclear Physics. New York: Cambridge UP, 2001.

9. Turner, James E. Atoms, Radiation, and Radiation Protection. New York: Wiley-Interscience, 1995.

10. Genie 2000. Computer software. Vers. 3.1A. Meriden, CT: Canberra, 2006.